INTERNATIONAL JOURNAL OF AUTOMOTIVE AND MECHANICAL ENGINEERING (IJAME)
ISSN: 2229-8649 e-ISSN: 2180-1606
VOL. 17, ISSUE 2, 7858 – 7867
DOI: https://doi.org/10.15282/ijame.17.2.2020.05.0586

ORIGINAL ARTICLE

A Novel Boat Shock Vibration Control using Momentum Exchange Principle with Pre-Straining Spring Mechanism

Lovely Son[1*], Jhon Malta[1], Eka Satria[1], Berry Yuliandra[1] and Hiroshi Matsuhisa[2]

[1]Mechanical Engineering Department, Andalas University, Padang, Indonesia
[2]Kyoto University, Japan

ABSTRACT – This research proposes a new method for boat impact vibration attenuation using the exchange of momentum principle with a pre-straining spring mechanism. The boat dynamic is modelled using a hinged-supported beam structure. The wave excitation on the boat hull is expressed using one degree of freedom spring-mass system. The simulation study is performed to evaluate the impact damper performance in reducing the boat shock response. Two kinds of momentum exchange impact damper i.e., without and with pre-straining spring mechanism were evaluated. The simulation results show that the impact damper with pre-straining spring mechanism (PSMEID) is better than the passive momentum exchange impact damper (PMEID) in reducing the boat shock vibration response.

ARTICLE HISTORY
Revised: 22nd Apr 2020
Accepted: 29th June 2020

KEYWORDS
PSMEID, PMEID, Impact, Shock, Damper

INTRODUCTION

Shock induced vibration attenuation has become an important consideration in designing safe and comfortable vehicles such as cars, aeroplane, and marine boats [1-5]. In the case of a high-speed craft (HSC), shock excitation load is mainly caused by a collision between boat hull and wave [6-7]. Human body vibration caused by this type of shock load has been identified as one of the major causes of health problems among HSC crew [8]. The vibration effect on HSC passengers induces physical and mental fatigue [9,10] and chronic and acute injuries [11,12].

Several methods have been proposed to reduce the body vibration of HSC passengers, including the design of boat seat and operational model. A technique for marine boat motion mitigation using flexible hull design has been proposed by Towsend[13]. Cripps [14], develops a new crew seat system for high-speed rescue craft. Shock isolation of the human body and the seat interaction model is analysed by Coe [15].

The passive momentum exchange impact damper (PMEID) has been proposed to reduce the impact-induced vibration of several structural and mechanical systems [16,17]. Even though PMEID effective in reducing the impact acceleration response for large impact frequency, however, its performance decreases when the impact frequency closest to the main mass natural frequency [18].

The actuator has been used to improve the momentum exchange impact damper performance in reducing the response of shock vibration problems. This active momentum exchange impact damper (AMEID) can effectively reduce both acceleration and displacement response of the main system under impact load [19]. The main drawback of AMEID is that this control technique requires a large power actuator to get optimal control results.

The passive momentum exchange impact damper with additional pre-straining spring has been introduced to improve the momentum exchange mechanism during the impact time [20]. The application of this control technique in reducing the impact force transmission on UAV landing gear has been studied by Son [21]. In this study, the momentum exchange impact damper using pre-straining spring mechanism (PSMEID) was proposed to reduce the shock-induced vibration of HSC. The model of boat dynamic with impact damper is developed, and the governing equation of the system was numerically calculated using MATLAB software. An analysis was performed to evaluate the effectiveness of PSMEID in reducing the shock-induced vibration on the HSC model due to collision between boat hull and wave.

SHOCK VIBRATION CONTROL BY MOMENTUM EXCHANGE

Figure 1 shows the schematic representation of shock vibration control using PMEID and PSMEID. The first ball moves to the right side at a constant velocity. The second ball and the third ball are initially in contact condition. The first ball represents the impact source. The second ball is the main system that receives an impact load. The third ball serves as the impact damper and receives part of the second ball momentum. When the first ball collides with the second ball during short period time, part of its momentum is transferred to the third ball. Theoretically, the larger the contact stiffness, the more momentum is transferred from the second ball to the third ball. Therefore, for high impact frequency, the passive momentum exchange impact damper (PMEID), as shown in Figure 1(a) has an excellent performance in reducing the motion of the second ball.

*CORRESPONDING AUTHOR | Lovely Son | ✉ lovelyson@eng.unand.ac.id

In the case of low impact frequency, the effectiveness of PMEID decreases due to the amount of momentum exchange is reducing [18]. To improve the momentum exchange impact damper performance, a pre-straining spring mechanism is positioned between the second and the third ball, as shown in Figure 1(b). This type of impact damper is named the pre-straining spring momentum exchange impact damper (PSMEID). At the instant after the first ball collides with the second ball, the pre-straining spring is released and pushes the second ball to the left side. The reaction force from the pre-straining spring counteracts the impulsive excitation of the first ball. As a result, the second ball remains stationary after the impact.

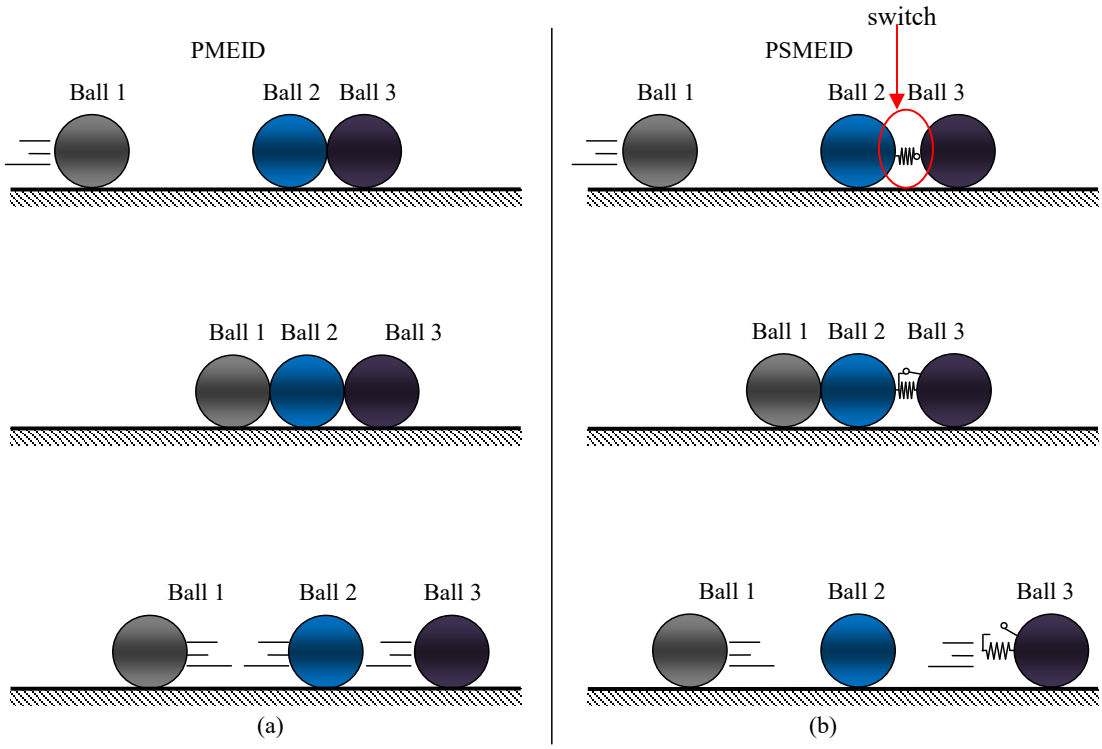

Figure 1. Shock vibration control by momentum exchange principle.

BOAT IMPACT VIBRATION MODEL WITH PSMEID

The boat impact vibration model with PSMEID is shown in Figure 2. The boat dynamics are modelled using a hinged-supported beam structure. Several methods can be used to derive the model of beam structure such as: exact model[22], identification model[23] and discrete model[24]. In this research, the discrete model of beam structure is derived using finite element method.

The PSMEID is represented by a contact mass m_c and a damper mass, m_d, that connected each other by a pre-straining spring k_{ps}. The initial displacement, x_{ps}, is applied to the pre-straining spring. A counteracting force, f_t, balances the pre-straining spring force due to the initial displacement. The mechanical switch mechanism releasing the counteracting force after the beam collides with the wave. The contact mass is contacting with the beam via a contact spring, k_{cd}, and contact damping, c_{cd}. The wave model is represented using a one DOF vibration system. m_w, and k_w, are the wave mass and stiffness, respectively. The contact model between the wave mass and beam is described by using the contact spring, k_{cw}, and contact damping, c_{cw}. The governing equations of the boat impact vibration model with PSMEID are written as:

$$\boldsymbol{M_s\ddot{u} + C_s\dot{u} + K_s u = B_d f_d - B_w f_w - B_g f_g} \tag{1}$$

$$m_d\ddot{z} + c_d\dot{z} + k_d z + f_{ps} + f_t = 0 \tag{2}$$

$$m_c\ddot{y} + f_d - f_{ps} - f_t = 0 \tag{3}$$

$$m_w\ddot{x} + c_w\dot{x} + k_w x - f_w = 0 \tag{4}$$

$\boldsymbol{M_s}$, $\boldsymbol{C_s}$ and $\boldsymbol{K_s}$ represent the beam structure mass, damping, and stiffness matrices. $\boldsymbol{u}$ is the displacement of the beam structure, and subscript d, w, g illustrates the symbol of three external forces on the beam. The impulsive force, f_w, that acts on the beam comes from the collision between the wave mass, m_w, and beam structure. The damper force, f_d, is the reaction force from impact damper due to the collision between the beam and the wave mass. The external excitation force applied to the beam is expressed by:

$$f_w = \begin{cases} 0, for\ u_w - x > 0 \\ k_{cw}(u_w - x) + c_{cw}(\dot{u}_w - \dot{x}), for u_w - x \le 0 \end{cases} \quad (5)$$

The contact force between the beam and the contact mass is given by:

$$f_d = \begin{cases} 0, for\ y - u_d > 0 \\ k_{cd}(y - u_d) + c_{cd}(\dot{y} - \dot{u}_d), for y - u_d \le 0 \end{cases} \quad (6)$$

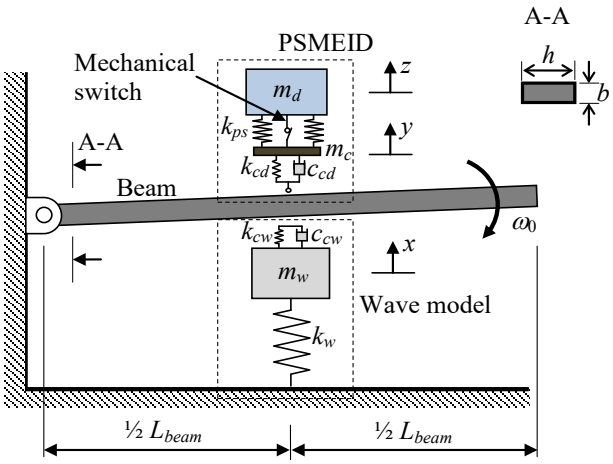

Figure 2. Boat impact vibration model with PSMEID.

f_g and f_{ps} in Eq.(1) and (2) are the gravitational force of the beam and the pre-straining spring force which is given by:

$$f_g = m_{beam} g \quad (7)$$

$$f_{ps} = k_{ps}(z - y - x_{ps}) \quad (8)$$

Where m_{beam} is the beam mass. $\mathbf{B_d}$, $\mathbf{B_w}$, and $\mathbf{B_g}$ in Eq.(1) are vectors describing the position of the external forces on beam structure. These vectors are given by:

$$\boldsymbol{B_d} = \{\delta_{dofd,1} \quad \delta_{dofd,2} \cdots \delta_{dofd,j} \cdots \quad \delta_{dofd,NDOF}\}^T \quad (9)$$

$$\boldsymbol{B_w} = \{\delta_{dofw,1} \delta_{dofw,2} \cdots \delta_{dofw,j} \cdots \quad \delta_{dofw,NDOF}\}^T \quad (10)$$

$$\boldsymbol{B_g} = \{\delta_{dofg,1} \quad \delta_{dofg,2} \cdots \delta_{dofg,j} \cdots \quad \delta_{dofg,NDOF}\}^T \quad (11)$$

dofd, *dofw*, and *dofg* in Eq.(9) to Eq.(11) denote the location of the external forces f_d, f_w and f_g on beam, respectively. $\delta_{i,j}$ is a delta function that can be expressed as:

$$\delta_{i,j} = \begin{cases} 1, i = j \\ 0, i \ne j \end{cases} \quad (12)$$

By using the modal analysis technique, the governing equation of beam vibration in Eq.(1) can be written as[19]:

$$\ddot{q}_i + 2\zeta_i \omega_i \dot{q}_i + \omega_i^2 q_i = \psi_i \left[\boldsymbol{B_d} f_d - \boldsymbol{B_w} f_w - \boldsymbol{B_g} f\right], \mathrm{i} = 1,2,\cdots,\infty, \quad (13)$$

The displacement and velocity response of the beam structure is calculated numerically from the equations of motion of the system using the Rungge-Kutta (RK) Dorman-Prince method. In this method, the equations of motion in Eq.(2), (3), (4), and (13) are written in a state-space form as follows:

$$\frac{d\boldsymbol{x}}{dt} = \dot{\boldsymbol{x}}(t) = f(t, \boldsymbol{x}(t)), \boldsymbol{x}(t_0) = \boldsymbol{x}_0 \quad (14)$$

The numerical solution to the general ordinary differential equation (ODE) problems using Dorman-Prince method takes the form:

$$k_1 = hf(t_k, x_k)$$

$$k_2 = hf\left(t_k + \frac{1}{5}h, x_k + \frac{1}{5}k_1\right)$$
$$k_3 = hf\left(t_k + \frac{3}{10}h, x_k + \frac{3}{40}k_1 + \frac{9}{40}k_2\right)$$
$$k_4 = hf\left(t_k + \frac{4}{5}h, x_k + \frac{44}{45}k_1 - \frac{56}{15}k_2 + \frac{32}{9}k_3\right)$$
$$k_5 = hf\left(t_k + \frac{8}{9}h, x_k + \frac{19372}{6561}k_1 - \frac{25360}{2187}k_2 + \frac{64448}{6561}k_3 - \frac{212}{729}k_4\right)$$
$$k_6 = hf\left(t_k + h, x_k + \frac{9017}{3168}k_1 - \frac{355}{33}k_2 - \frac{46732}{5247}k_3 + \frac{49}{176}k_4 - \frac{5103}{18656}k_5\right)$$
$$k_7 = hf\left(t_k + h, x_k + \frac{35}{384}k_1 + \frac{500}{1113}k_3 + \frac{125}{192}k_4 - \frac{2187}{6784}k_5 + \frac{11}{84}k_6\right)$$

The next step value x_{k+1} is calculated as follows:

$$x_{k+1} = x_k + \frac{35}{384}k_1 + \frac{500}{1113}k_3 + \frac{125}{192}k_4 - \frac{2187}{6784}k_5 + \frac{11}{84}k_6 \tag{15}$$

Where h is the step time used in the numerical simulation.

RESULTS AND DISCUSSION

The simulation study was conducted to evaluate the PSMEID performance in reducing the boat shock vibration response. In this research, the evaluation was performed by comparing the maximum transient response amplitude of the boat. Numerical simulation using RK Dorman-Prince method is utilised to solve Eq.(2), (3), (4), and (13). The simulation is performed numerically using MATLAB software. The displacement and velocity responses were calculated using Eq.(15). The beam dynamics is analysed using modal analysis by considering only five lowest modes of the beam. The ship-wave interaction during impact is simulated by giving the initial velocity to the beam when contacting the wave mass.

For a comparison study, the boat model without and with passive momentum impact damper (PMEID), as shown in Figure 3 are also simulated. As shown in Figure 3, the external contact forces f_d and f_w are acting at the centre of the beam. The beam material is assumed homogeneous; therefore, the location of the beam centre of mass is similar to its centre of geometry. The displacement, velocity, and acceleration response are calculated at the free tip of the beam.

Table 1 shows the parameters used in the simulation. In the simulation study, the initial angular velocity of the beam is ω_0 = 1 rad/s. The initial linear velocity at the centre of the beam that relating to this initial angular velocity is $v_0 = 0.5\ \omega_0 L_{beam}$. The pre-straining spring stiffness k_{ps} is determined using the results from an author's previous study [20]:

$$k_{ps} = 0.25 m_d \omega_w^2 \tag{16}$$

ω_w is the wave excitation frequency. This excitation frequency is given by:

$$\omega_w = \sqrt{\frac{k_{cw}}{m_w}} \tag{17}$$

The excitation period can be written as:

$$T_w = \frac{2\pi}{\omega_w} \tag{18}$$

The optimum initial deflection of the pre-straining spring is calculated as follows:

$$x_{ps} = \frac{0.63 F_w}{k_{ps}} \tag{19}$$

F_w in Eq.(19) is the amplitude of the excitation force.

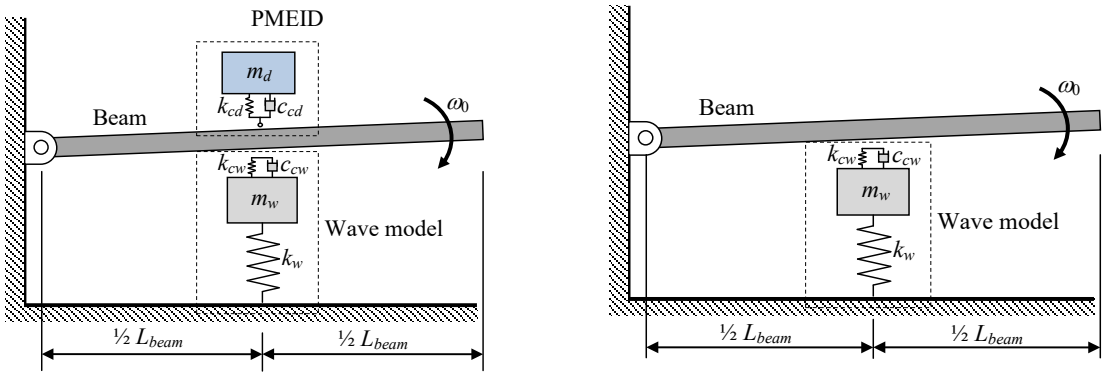

Figure 3. Boat impact vibration model with PMEID and without damper

Table 1. Simulation parameters

No	Parameters	Value	Unit
1	Beam mass density, ρ_{beam}	8400	kg/m^3
2	Elastic modulus of the beam	120×10^9	N/m^2
3	Beam Length, L_{beam}	0.6	M
4	Beam width, b	0.06	M
5	Beam thickness, h	0.008	M
6	Damper mass, m_d	0.012	Kg
7	Contact mass, m_c	0.12×10^{-3}	Kg
8	Wave mass, m_w	0.1	Kg
9	Damper contact stiffness, k_{cd}	5×10^6	N/m
10	Damper contact damping, c_{cd}	80	N.s/m
11	Wave contact stiffness, k_{cw}	5×10^5	N/m
12	Wave contact damping, c_{cw}	0	N.s/m
13	Pre-straining spring stiffness, k_{ps}	3×10^5	N/m
14	Wave stiffness, k_w	2000	N/m

Figure 4 shows the frequency response function (FRF) of the beam structure. The frequency response function is obtained with the excitation point located at the centre of the beam, and the response is calculated at the free tip of the beam. As shown in Figure 4, four peak frequencies are located between 0 to1000 Hz. These peaks are relating the 2nd, 3rd, 4th, and 5th natural frequencies of the beam. These frequencies are the four lowest elastic modes of the beam. The first beam natural frequency at 0 Hz is relating to the beam rigid body mode. Four lowest mode shapes of the beam are drawn schematically in Figure 5. Table 2 shows the four lowest mode shapes of the beam structure and its corresponding natural frequencies. As shown in Table 2, the first natural frequency at 0 Hz is relating to the rigid body mode of the beam.

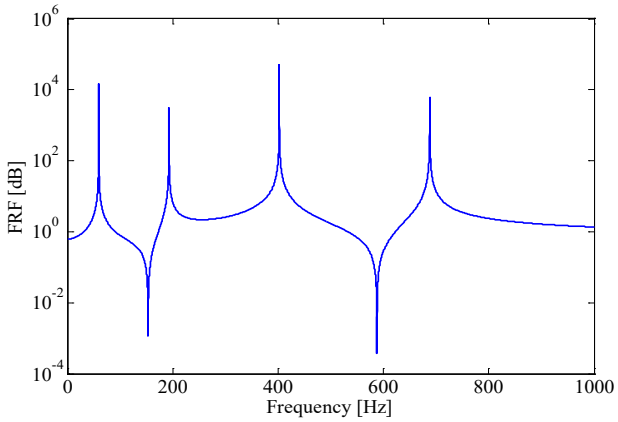

Figure 4. FRF of the beam structure

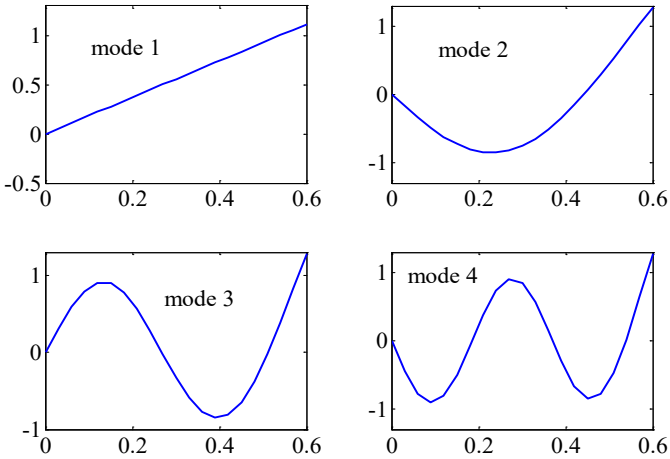

Figure 5. Four lowest mode shape of the beam structure.

Table 2. Natural frequency of the beam.

No	Modes	Frequency (Hz)
1	Mode 1	0
2	Mode 2	59.5
3	Mode 3	192.8
4	Mode 4	402.3
5	Mode 5	688.0

The impact responses of the beam for three conditions, i.e.; without a damper, with PMEID and PSMEID were evaluated. In the simulation, the mechanical switch was released after $0.1T_w$ [20]. Figure 6(a) shows the displacement, velocity, and acceleration response of the beam using small damper mass ($m_d = 0.005\ m_{beam}$). The beam response using large damper mass($m_d = 0.05\ m_{beam}$) is shown in Figure 6(b). As shown in Figure 6(a) and 6(b), the maximum velocity and acceleration response obtained using PSMEID are smaller than those obtained using PMEID. The reason is that, in the PMEID, the impact force received by the beam from the wave is directly transferred to the impact damper mass. However, due to the impact damper mass is much smaller than the beam mass, the momentum exchange between the beam and the damper mass is small. In the PSMEID, the exchange of momentum between impact damper mass and the beam is large because of the pre-straining spring mechanism. In this case, the pre-straining spring simultaneously releases and push the beam after impact. As a result, the velocity and acceleration response of beam using PSMEID is smaller than those obtained using PMEID.

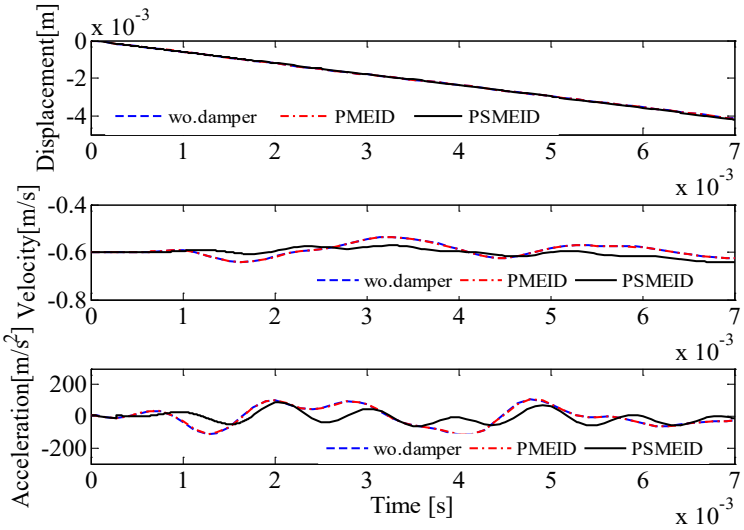

(a) $m_d = 0.005\ m_{beam}$

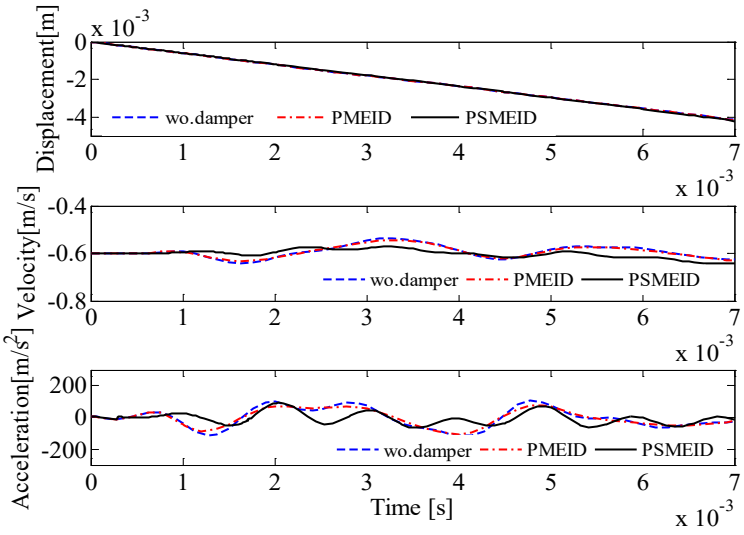

(b) $m_d = 0.05\ m_{beam}$

Figure 6. Time response of the beam using small damper mass.

Figure 7 shows the contact forces and the damper mass velocity during and after the impact time. As shown in Figure 7, the excitations force F_w is a half sinusoidal function with period $T_w = 2.8$ ms. The contact force from the impact damper F_d acts after the mechanical switch is released at $t = 0.28$ ms. After this releasing time, the damper mass velocity increases from zero to a constant value $v_d = 2.4$ m/s. These results indicate that a large amount of momentum is transferred from the beam to the impact damper mass, and the beam response decreasing after the mechanical switch releases.

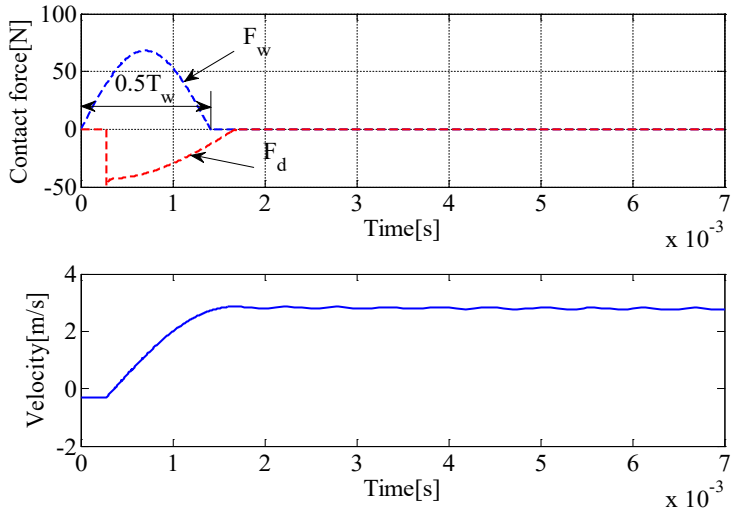

Figure 7. Contact force and velocity of m_d.

The frequency response of displacement, velocity, and acceleration of the beam is shown in Figure 8. It is shown in Figure 8 that the displacement and velocity response has a significant amplitude in the frequency range lower than 200 Hz. Meanwhile, the acceleration response has wider frequency content in comparison with the displacement and velocity responses. The results depicted in Figure 8 have shown that PSMEID produces high-frequency components in the acceleration response of the beam. These high-frequency components can be reduced by increasing the beam damping factor.

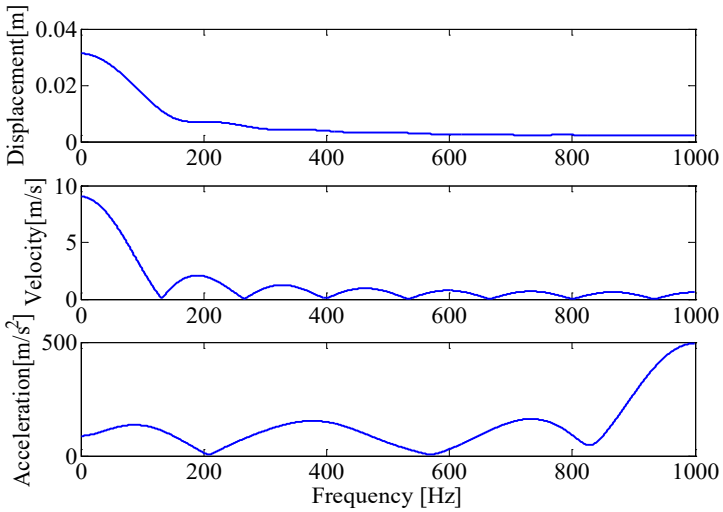

Figure 8. The frequency response of the beam using small damper mass ($m_d = 0.005\ m_{beam}$).

Figure 9 shows a comparison of the largest acceleration ratio obtained using PMEID and PSMEID versus variation of the damper mass. The acceleration ratio is a ratio of the maximum acceleration peak obtained with and without impact damper. It is shown in Figure 9 that the maximum beam acceleration ratio using PSMEID is lower than that obtained using PMEID for damper mass ratio between 0.05 to 0.25. According to this result, it can be concluded that PSMEID performance is better than PMEID for the mass ratio larger than 0.05.

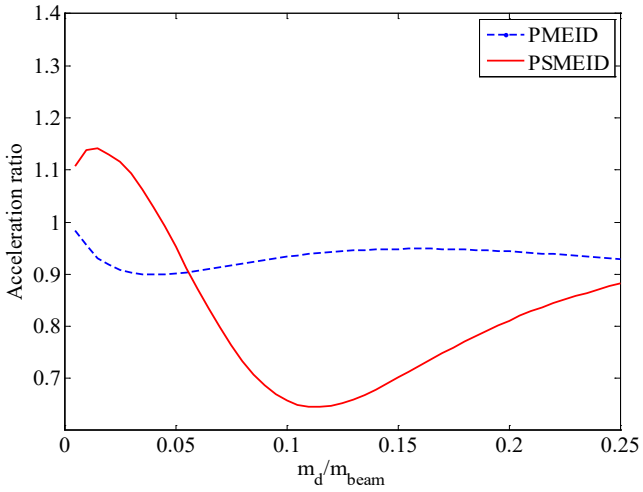

Figure 9. Acceleration ratio with PMEID and PSMEID.

The influence of the damper position to the maximum acceleration response of the beam is shown in Figure 10. According to the result depicted in Figure 10, it can be observed that the best position for the impact damper is located at the centre of the beam.

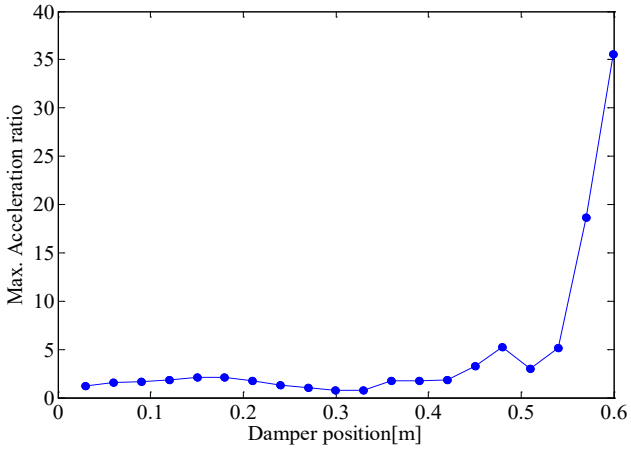

Figure 10. Acceleration ratio vs. damper position

CONCLUSION

The simulation results of boat shock vibration control using impact damper have shown that PSMEID can reduce the boat maximum velocity and acceleration responses due to the pre-straining spring mechanism. This result can improve boat passenger safety and comfort during the collision between boat hull and wave. Furthermore, it was shown that PSMEID performance is better than that of PMEID for damper mass ratio larger than 0.05. The simulation study has shown that the optimal position for impact damper is located at the centre of the boat.

AKNOWLEDGEMENT

Financial support from the acceleration of professor research scheme No: 6/UN.16.17/PP.PGB/LPPM/2018, Andalas University year 2018 is gratefully acknowledged.

REFERENCES

[1] Sakaray U, O'Toole BJ, Trabia MB, Thota J. Optimization of a vehicle space frame under ballistic impact loading. In : ASME 2007 International Design Engineering Technical Conferences Computers and Information in Engineering Conference, Las Vegas, USA, pp. 317-324; 2007

[2] Adam SA, Jalil NAA, Razali KAM, Ng YG, Aladdin MF. Mathematical model of suspension seat-person exposed to vertical vibration for off-road vehicles. International Journal of Automotive and Mechanical Engineering (IJAME), 2019; 16(2): 6773-6782.

[3] Aladin MF, Jalil NAA, Guan NY, Rezali KAM, Adam SA. Evaluation of human discomfort from combined noise and whole-body vibration in passenger vehicle. International Journal of Automotive and Mechanical Engineering (IJAME), 2019; 16(2): 6808-6824.

[4] Chopra S, Nawani S, Bisht K. FEM analysis of landing gear strut. International Journal of Aerospace and Mechanical Engineering, 2015; 2(1):1-3

[5] Lernbeiss L, Plochl M. Simulation model of an aircraft landing gear considering elastic properties of the shock absorber. Journal of Multi-body Dynamics, 2007; 221:77-86.

[6] Allen D, Taunton D, Allen R. A study of shock and vibration dose values on board high-speed marine craft. International Journal of Maritime Engineering, 2008; 150(A3):1-10.

[7] Peterson R, Pierce E, Price B, Bass C. Shock mitigation for the human on high speed craft: development of an impact injury design rule. In: RTO AVT Symposium on Habitability of combat and transport vehicles: noise, vibration and design, Prague, Czech, pp. 31-1-31-14; 2004.

[8] Mansfield NJ. Vibration and shock in vehicles: new challenges, new methods, new solutions. In: 1st International Comfort Congress, Salerno, Italy, pp. 6769-1721; 2017.

[9] Lemmer P. Rib development design and construction. In: International Conference on Rigid Inflatables RINA, Weymouth, UK; 1998.

[10] Myers S, Dobbins T, King S. Hall B, Ayling R, Holmes S, Gunston T, Dyson R. Physiological consequences of military high-speed boat transits. Eur.J.App. Physiol, 2011; 111(9): 2041-2049.

[11] Troesch A, Falzarano, JM. Modern nonlinear dynamical analysis of vertical plane motion of planning hulls. J. Ship Res, 1993; 37(3) : 189-199.

[12] Peterson R, Wyman D, Frank C. Drop test to support water impact and planning boat dynamic theory. United States Navy CSS/TR-97/25; 1997.

[13] Townsend NC, Coe TE, Wilson RA. Shenoi RA. High-speed marine craft motion mitigation using flexible hull design. Ocean Engineering, 2012; 42: 126-134.

[14] Cripps R, Rees S, Phillips H, Cain C, Richards D, Cross J. Development of a crew seat system for high speed rescue craft. In: FAST 2003, Naples, Italy; 2003.

[15] Coe T, Xing J, Shenoi RA, Taunton D. A simplified 3-d human body-seat interaction model and its applications to the vibration isolation design of high speed marine craft. Ocean Engineering, 2009; 36:732-746.

[16] Son L, Kawachi M, Matsuhisa H. Reducing floor impact vibration and sound using a momentum exchange impact damper. Journal of system design and dynamics, 2007; 1(1):14-26.

[17] Son L, Nakatani D, Matsuhisa H, Utsuno H. Application of Momentum Exchange Impact Dampers to Forging Machine. Journal of system design and dynamics, 2008; 2(4):1027-1039.

[18] Son L, Matsuhisa H, Utsuno H. Energy Transfer in a three body momentum exchange impact damper. Journal of system design and dynamics, 2008; 2(1):425-441.

[19] Son L, Bur M, Rusli M. Experiment of shock vibration control using active momentum exchange impact damper. Journal of Vibration and Control, 2010; 16(1):49-64.

[20] Son L, Bur M, Rusli M, Matsuhisa M, Yamada K, Utsuno H. Fundamental study of momentum exchange impact damper using pre-straining spring mechanism. International Journal of Acoustic and Vibration, 2017; 22(4):422-430.

[21] Son L, Bur M, Rusli M. A new concept for UAV landing gear shock vibration control using pre-straining spring momentum exchange impact damper. Journal of Vibration and Control, 2018; 24(8):1455-1468.

[22] Tamer AES, Said HF. Exact vibration of Timoshenko beam combined with multiple mass spring sub-systems. Structural Engineering and Mechanics, 2016; 57(6) : 989-1014.

[23] Rahman TAZ, As'arry A, Jalil NAA, Kamil R. Dynamic modelling of a flexible beam structure using feedforward neural networks for actice vibration control. International Journal of Automotive and Mechanical Engineering (IJAME), 2019; 16(1): 6263-6280.

[24] Chaphalkar SP, Subhash N, Khetre N, Arun MM. Modal analysis of cantilever beam structure using finite element analysis and experimental analysis. American journal of engineering research, 2015; 4(10):178-185.